

Virtual source gathers and attenuation of free-surface multiples using OBC data: implementation issues and a case study

Kurang Mehta¹, Roel Snieder¹, Rodney Calvert² & Jonathan Sheiman²

¹Center for Wave Phenomena, Department of Geophysics, Colorado School of Mines, Golden, CO 80401

²Shell International Exploration and Production Inc., 3737 Bellaire Blvd. Houston, TX 77001

Summary

Virtual source imaging is a technique based on extracting the Green's function that characterizes wave propagation between two receivers by cross-correlating the wave-fields recorded at these receivers and summing over all sources. Implementation issues in generating a virtual source gather include the choice of the receiver that acts as the virtual source and the number of sources over which the cross-correlated data is stacked. By stacking over specific source locations, we generate virtual source gathers containing waves within a specified horizontal slowness interval. Artifacts due to the traces at the edges of the source aperture need to be suppressed by applying a taper before stacking. We use dual-sensor summation to separate the up- and the down-going energy in the raw data. We use this to generate virtual source gathers containing only the up-going energy, hence attenuating the free-surface multiples.

Introduction

Virtual source imaging (Lobkis and Weaver, 2001; Derode, et al., 2003; Bakulin and Calvert, 2004; Calvert, et al., 2004; Schuster, 2004; Snieder, 2004; Wapenaar, 2004; Wapenaar, et al., 2005) is a technique based on extracting the Green's function that characterizes the wave propagation between any two pair of receivers by cross-correlating the recorded wave-fields. An important advantage of virtual source imaging is that the wave-field recorded by the two receivers can be generated either by active sources or by incoherent sources (e.g., Sabra, et al., 2005; Shapiro, et al., 2005).

We generate virtual source gathers by cross-correlating the wave-field recorded at a reference receiver (virtual source) with the wave-field recorded at all the other receivers, and stacking over sources. Virtual source gathers containing waves within a specified horizontal slowness interval can be generated using suitable combination of receiver acting as the virtual source and the sources used for stacking. We apply this to a 4-C OBC data recorded at the Mars field. Fig. 1 shows a cartoon of the acquisition geometry. It consists of 360 shots (spaced every 25 m) on the sea-surface with 120 4-C sensors (spaced every 50 m) permanently stationed on the sea-floor 1 km deep. As shown in Fig. 1 these 360 shots are divided into 9 panels. The horizontal bar in shot panel 7 indicates missing shots. Fig. 2 shows hydrophone component of a raw shot gather. It depicts a direct arrival (A) that propagates with the water velocity (1500 m/s), refractions (B) and reflections (C). The group of events marked by D

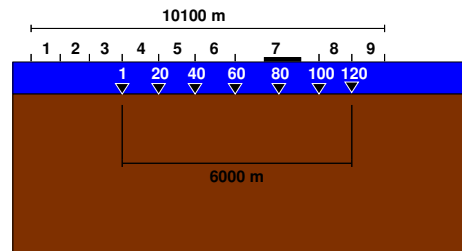


Fig. 1: Cartoon of the acquisition geometry of the ocean-bottom cable data set obtained from the Mars field.

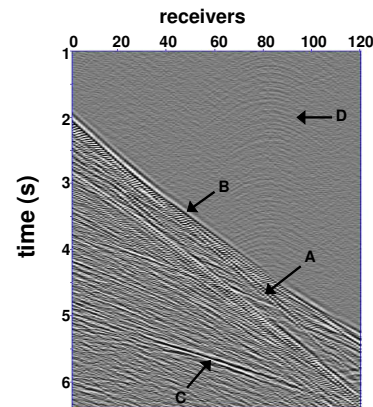


Fig. 2: A single raw shot gather recorded by the hydrophone.

correspond to the noise because of a service boat for the platform.

In the next section we describe the generation of the virtual source gathers and focus on restricting the direction of the incoming energy to generate virtual source gathers containing arrivals within a specified horizontal slowness interval. We diagnose edge-effects in the virtual source gather and apply dual-sensor summation to the virtual source gathers to attenuate the free-surface multiples.

Generation of Virtual Source Gathers

Stationary phase analysis is one approach to diagnose the source locations that give a stationary phase contribution (Wapenaar, et al., 2005; Snieder, et al., 2006). Fig. 3(a) shows a correlation gather with each trace representing the cross-correlation of the waves recorded at receiver 1 with the waves recorded at receiver 120 for a given source location. The arrival times of the waves in the correla-

Virtual Source Gatherers

tion gather has two peaks (boxes 1 & 2) corresponding to two stationary phase points. The arrow indicates a discontinuity in the correlation gather that is caused by the missing shots in source panel 7. We generate similar correlation gathers by cross-correlating receiver 1 (virtual source) with every other receivers. To generate a virtual source gather, we stack the correlation gathers over all the sources. In the stack, the non-zero contribution is due to the physical sources (boxes 1 & 2) that are near the stationary path. Instead of stacking over all sources, we can also stack over a sub-set that include the sources that give a stationary phase contribution. The ability to stack over different panels of sources can be used to separate waves travelling with different horizontal slownesses.

Wave-field separation

If instead of stacking over all the sources, we stack the correlation gather over source panel 3 (shown in Fig. 1) that gives a stationary phase contribution, we obtain virtual source gather as shown in Fig. 3(b). Most of the arrivals are reflections either from the subsurface or from the free-surface. If we stack over only source panel 3, we restrict the direction of the incoming energy. Virtual source gathers generated by stacking over a specific set of sources can, hence, be used to separate the waves propagating with different horizontal slownesses. The arrival close to the direct arrival for near offset, highlighted by an ellipse, is an artifact that is caused by edge-effects associated with truncation of the stack over finite number of shots. We address this edge-effect in the subsequent section. Fig. 3(b) also show three strong events occurring at 1.4, 2.8 and 4.2 s that are marked by letters A, B and C respectively. These arrivals correspond to the free-surface multiples.

Suppression of free-surface multiples

Since we have both the hydrophone (H) and vertical geophone (Z) recording, we use dual-sensor summation (e.g., Jiao, et al., 1998; Barr, et al., 1996; Dragoset and Barr, 1994; Ball and Corrigan, 1996; Canales and Bell, 1996; Soubaras, 1996; Loewenthal and Robinson, 2000; Robinson, et al., 1999) to separate the up- (given by H+Z) and the down-going waves (given by H-Z). Before we take the sum and difference of the hydrophone and the vertical geophone, we calibrate the vertical geophone to the hydrophone. For the virtual source gather in Fig. 3(b), we correlated the entire wave-field resulting in a virtual source gather containing both the up-going and the down-going energy. If instead, we correlate the hydrophone recording at the virtual source with the H+Z wave-field (down-going energy) at all the other receivers, we obtain the virtual source gather with mainly up-going energy as shown in Fig. 3(c). The direct arrival is attenuated and so are the free-surface multiples. Since this virtual source gather consists mainly of the up-going energy, we see reflections from the subsurface. Hence, using the dual-sensor summation, we can separate the up-going and the down-going waves to isolate the reflections from the sub-

surface and suppress free-surface multiples. Fig. 3(c) contains incoherent jitter in the near-offset which is not present when the full wave-field of the hydrophone is used for cross-correlation [Fig. 3(b)]. Hence, the incoherent energy is due to the contribution of the vertical component geophone. Schalkwijk, et al. (2003) studied a similar decomposition of multicomponent ocean-bottom seismic waves into down-going and up-going energy. They explain this jitter as the cross-coupling of the vertical component with the horizontal components.

Artifacts in virtual source gathers

One of the artifacts in virtual source gathers is the effect of sources at the two edges of the aperture while stacking over the sources. To illustrate this edge-effect, we consider the virtual source gather for hydrophone with receiver 60 as the virtual source [Fig. 4(a)]. The correlation gather is stacked over the sources in panel 5 because they give the stationary phase contribution. The wave-field for time $t > 0$ and offset to the right of receiver 60 consists mainly of the direct arrival and a strong reflection (D). The wave-field for $t < 0$ and offset to the left of receiver 60, however, is different. Box A highlights spurious arrivals that are caused because we stack the correlation gather over a small sub-set of sources. We show later that these spurious events average out by using a larger source aperture such that energy comes from all possible directions. The weak arrivals marked by B have move-out parallel to the direct arrival and correspond to the side-lobes of the auto-correlation of the source-time function. These artifacts can be removed by deconvolving all the traces in the correlation gather with the power spectrum of the source signal. The direct arrival extends to negative times to give two spurious arrivals shown by C. These spurious arrivals correspond to the edge-effect while stacking over the sources with a limited aperture. The travel-time difference curve, representing the difference of the travel-time for wave-field to travel from the two end sources in panel 5 to receiver 60 and to the receivers 1 through 59 using the water velocity as 1500 m/s, agrees well with the kinematics of the artifact due to the edge-effect and hence, is a good diagnostic for estimating the shape of the artifact caused by the edge-effect. A simple way to attenuate the edge-effect is to taper the cross-correlated data or stack over a larger source aperture. We show in Fig. 4(b) that applying linear taper results in a virtual source gather without the artifacts due to edge-effects. In addition to the reflection event (D) for time $t > 0$ and offset to the right of receiver 60, due to the waves that arrive receiver 60, gets reflected and then arrives at other receivers, there is also a reflection (E) for $t < 0$ and offset to the left of receiver 60, which is because of the waves that gets reflected and then arrives at receiver 60.

If, instead of using only the source panel 5, we use all the sources (larger aperture) for stacking, we get the virtual source gather shown in Fig. 4(c). Since energy is coming from a larger range of directions, the reflections [D and E in Fig. 4(a)] at ± 1.4 s are now visible for both the

Virtual Source Gatherers

negative and positive offsets and times. Also the artifacts due to stacking over a small sub-set of sources [A in Fig. 4(a)] and edge-effect [C in Fig. 4(a)] have been suppressed by using a larger source aperture.

Conclusions

We show that the stack over a selected panel of source locations allow us to separate waves arriving with different horizontal slownesses. The free-surface multiples can be attenuated using the dual-sensor summation to separate the up-going and the down-going waves. In the process of generating the virtual source gatherers, to suppress the edge effects, it is important to apply tapering to the traces at the end before stacking the correlation gather. We show that the artifacts due to the edge effects can be diagnosed using the travel-time difference curve for the sources at the two ends of the aperture. Another artifact arises due to the side-lobes of the auto-correlation of the source-time function and can be removed by deconvolving all the traces in the correlation gather with the power spectrum of the source signal.

Acknowledgments

We thank the Gamechanger program of Shell International Exploration and Production Inc. for financial support.

References

- Bakulin, A., and Calvert, R., 2004, Virtual source: new method for imaging and 4D below complex overburden: 74th Ann. Internat. Mtg., Soc. Expl. Geophys., Expanded Abstracts, 2477–2480.
- Ball, V., and Corrigan, D., 1996, Dual-sensor summation of noisy ocean-bottom data: 66th Ann. Internat. Mtg., Soc. Expl. Geophys., Expanded Abstracts, 28–31.
- Barr, F. J., Paffenholz, J., and Rabson, W., 1996, The dual-sensor ocean-bottom cable method: Comparative geophysical attributes, quantitative geophone coupling analysis and other recent advances: 66th Ann. Internat. Mtg., Soc. Expl. Geophys., Expanded Abstracts, 21–22.
- Calvert, R. W., Bakulin, A., and Jones, T. C., 2004, Virtual Sources, a new way to remove overburden problems: 66th Mtg.: Eur. Assn. Geosci. Eng., P234.
- Canales, L., and Bell, M. L., 1996, Ghost attenuation using dual sensor cable data: 66th Ann. Internat. Mtg., Soc. Expl. Geophys., Expanded Abstracts, 1591–1594.
- Derode, A., Lacrose, E., Campillo, M., and Fink, M., 2003, How to estimate the Green's function for a heterogeneous medium between two passive sensors? Application to acoustic waves: Applied Physics Letters, **83**, 3054–3056.
- Dragoset, W., and Barr, F. J., 1994, Ocean-bottom cable dual-sensor scaling: 64th Ann. Internat. Mtg., Soc. Expl. Geophys., Expanded Abstracts, 857–860.
- Jiao, J., Trickett, S., and Link, B., 1998, Robust summation of dual-sensor ocean-bottom cable data: 68th Ann. Internat. Mtg., Soc. Expl. Geophys., Expanded Abstracts, 1421–1424.
- Lobkis, O. I., and Weaver, R. L., 2001, On the emergence of the Green's function in the correlations of a diffuse field: Journal of Acoustical Society of America, **110**, 3011–3017.
- Loewenthal, D., and Robinson, E. A., 2000, On unified dual fields and Einstein deconvolution: Geophysics **65**, 293–303.
- Robinson, E. A., Ewing, M., and Worzel, J. L., 1999, Seismic Inversion and Deconvolution. Part B: Dual-sensor technology: Pergamon-Elsevier, Amsterdam, The Netherlands.
- Sabra, K. G., Gerstoft, P., Roux, P., and Kuperman, W. A., 2005, Extracting time-domain Green's function estimates from ambient seismic noise: Geophysics Research Letters, **32**, L03310, doi:10.1029/2004GL021862.
- Schalkwijk, K. M., Wapenaar, C. P. A., and Verschuur, D. J., 2003, Adaptive decomposition of multicomponent ocean-bottom seismic data into downgoing and upgoing P- and S-waves: Geophysics, **68**, No.3, 1091–1102.
- Schuster, G. T., Yu, J., Sheng, J., and Rickett, J., 2004, Interferometric/daylight seismic imaging: Geophysics Journal International, **157** 838–852.
- Shapiro, N. M., Campillo, M., Stehly, L., and Ritzwoller, M. H., 2005, High-resolution surface-wave tomography from ambient seismic noise: Science, **307**, 1615–1618.
- Snieder, R., 2004, Extracting the Green's function from the correlation of coda waves: A derivation based on stationary phase: Physics Review E., **69**, 046610.
- Snieder, R., Wapenaar, K., and Larner, K., 2006, Spurious multiples in interferometric imaging of primaries: Geophysics, In Press.
- Soubaras, R., 1996, Ocean bottom hydrophone and geophone processing: 66th Ann. Internat. Mtg., Soc. Expl. Geophys., Expanded Abstracts, 24–27.
- Wapenaar, K., 2004, Retrieving the elastodynamic Green's function of an arbitrary inhomogeneous medium by cross-correlation: Physics Review Letters, **93**, 254301.
- Wapenaar, K., Fokkema, J., and Snieder, R., 2005, Retrieving the Green's function by cross-correlation: a comparison of approaches: Journal of Acoustical Society of America, **118**, 2783–2786.

Virtual Source Gathers

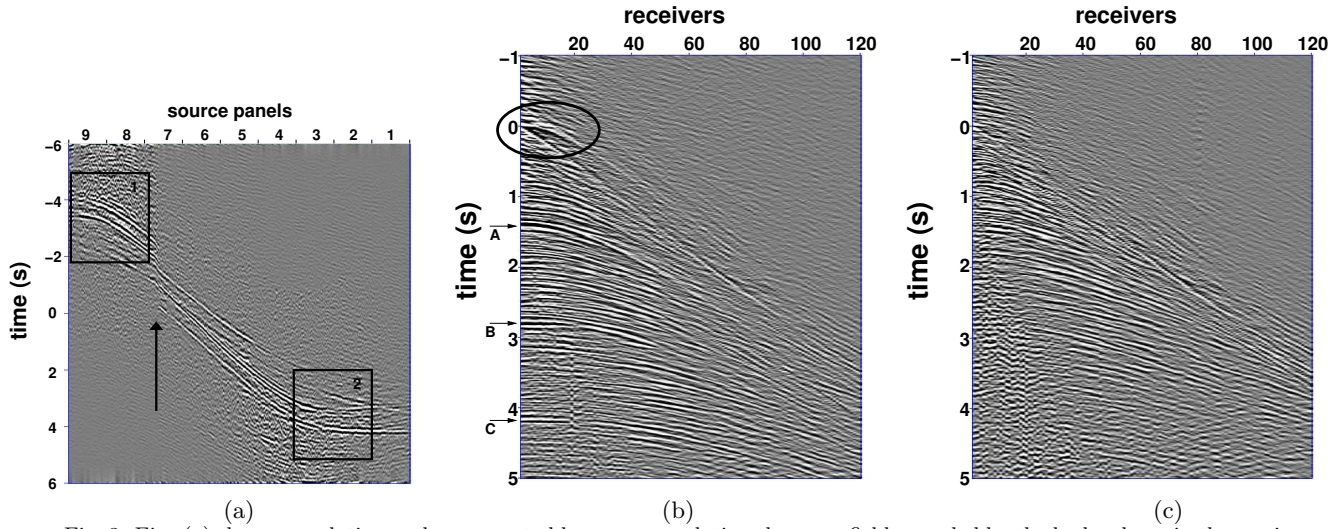


Fig. 3: Fig. (a) shows correlation gather generated by cross-correlating the wave-field recorded by the hydrophone in the receiver 1 with the wave-field recorded by the hydrophone in the receiver 120 for all source locations. Figs. (b) and (c) show virtual source gather with receiver 1 as the virtual source and source panel 3 used for stacking. In (b), the hydrophone wave-field recorded by receiver 1 (virtual source) is correlated with the hydrophone wave-field recorded by all other receivers and in (c), the hydrophone wave-field recorded by receiver 1 (virtual source) is correlated with the H+Z wave-field (down-going energy) recorded by all other receivers

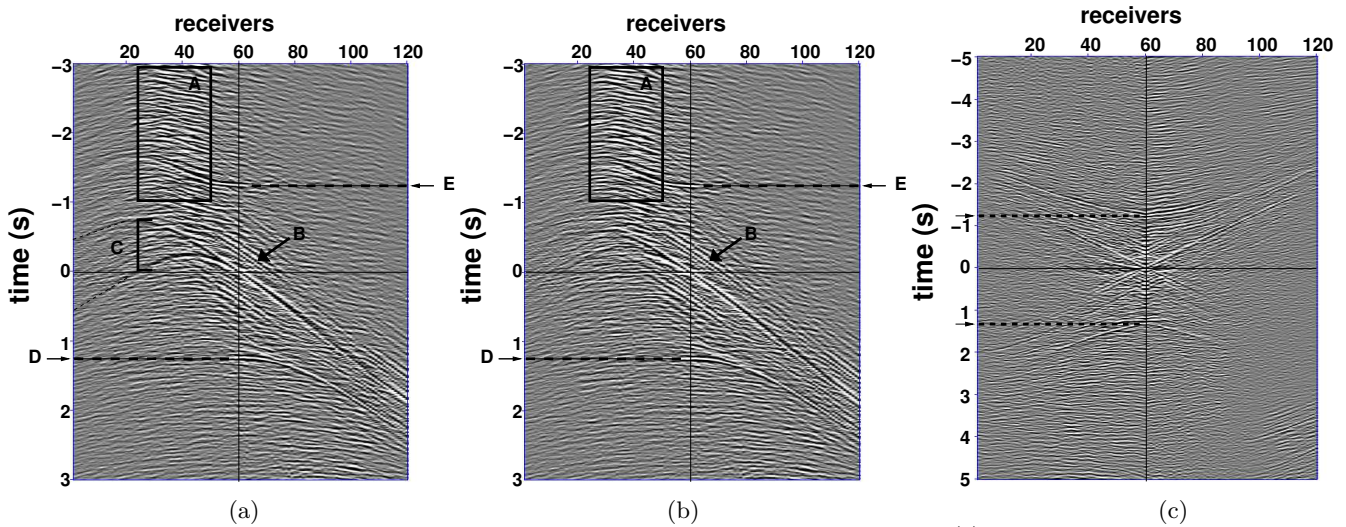


Fig. 4: Virtual source gather for hydrophone with receiver 60 as the virtual source and (a) source panel 5 used for stacking, (b) source panel 5 used for stacking and linear tapering applied at the end traces in the correlation gather, and (c) all source panels used for stacking.